Ab initio atomistic thermodynamics study on the selective oxidation mechanism of the surfaces of intermetallic compounds

Shi-Yu Liu,[1] Jia-Xiang Shang,[1,*] Fu-He Wang,[2] Shi-Yang Liu,[3] Yue Zhang,[1] and Hui-Bin Xu[1,†]

[1]*Key Laboratory of Aerospace Materials and Performance (Ministry of Education), School of Materials Science and Engineering, Beihang University, Beijing 100191, China*

[2]*Department of Physics, Capital Normal University, Beijing 100048, China*

[3]*Surface Physics Laboratory, Department of Physics, Fudan University, Shanghai 200433, China*

(Received 26 May 2009; revised manuscript received 25 July 2009; published 12 August 2009)

By combining *ab initio* density-functional theory and the thermodynamics calculations, we have constructed the surface phase diagrams (SPDs) for oxygen adsorption on the intermetallic compounds (IMCs) surfaces. Interestingly, from these SPDs, we can understand the selective oxidation behavior of IMCs surfaces easily and explains available experimental results successfully. Moreover, through a close examination of our results it can be found that two kinds of typical SPDs appear under O-rich conditions, i.e., a uniform single-phase SPD (type I) and a nonuniform double-phase SPD (type II) which correspond to the sustained complete selective oxidation and the nonsustained partial selective oxidation observed in the experiments. We believe that, using this general microscopic thermodynamics oxidation mechanism, one can easily judge and predict the oxidation behavior of arbitrary binary IMCs surfaces in the thermodynamics point of view.

DOI: 10.1103/PhysRevB.80.085414 PACS number(s): 68.35.Md, 68.43.Bc, 71.15.Mb, 81.65.Mq

I. INTRODUCTION

A thorough understanding of the oxidation occurring on the intermetallic compounds (IMCs) surfaces is of considerable fundamental interest and importance in the frontiers of a variety of different fields such as corrosion, passivation, and heterogeneous catalysis.[1,2] Specially, the IMCs such as NiAl, FeAl, γ-TiAl, and Nb_5Si_3 are drawing more and more attention due to the merits of low-mass density, excellent thermal conductivity, and high specific strength.[3,4] Moreover, in an oxidizing environment, some IMCs possess the excellent oxidation resistant resulting from the selective growth of a dense protective oxide layer such as Al_2O_3 or SiO_2 on their surfaces, which mainly depends on the stable selective oxidation of their surfaces.[5]

Because of the technological significance of the IMCs, many experiments were performed to understand the oxidation of NiAl(100), FeAl(100), γ-TiAl(111), and Nb_5Si_3 surfaces.[6–13] It is observed that although the clean NiAl(100) surface exhibit different structures, upon exposure to oxygen, the oxide formation is unaffected by its initial bare surface composition. The oxidation of NiAl(100) surface easily forms a continuous coherent Al_2O_3 film on the top of surface.[6–8] Similarly, the oxidation of FeAl(100) surface also forms a continuous coherent Al_2O_3 film easily on the top of the surface.[6,9] Obviously, NiAl(100) and FeAl(100) systems exhibit the sustained complete selective oxidation behavior on the their surfaces. However, for the oxidation of γ-TiAl(111) surface, a two-stage oxidation process is observed. At the first stage an ultrathin γ-like Al_2O_3(111) film on the γ-TiAl(111) surface was produced at 650 °C under low oxygen pressure resulting from the selective oxidation of aluminum.[10,11] Then, at the second stage a simultaneous oxidation of both metal elements is observed.[11] The similar two-stage oxidation process also occurs on the polycrystalline phase γ-TiAl surface.[12] For the oxidation of Nb_5Si_3 intermetallic alloys, the formation of main Nb_2O_5 and a little SiO_2 mixture is observed.[13] Accordingly, different from NiAl(100) and FeAl(100), γ-TiAl(111) and Nb_5Si_3 exhibit the nonsustained partial selective oxidation behavior on the surfaces.

Although some *ab initio* studies[14,15] were devoted to the understanding of the selective oxidation of IMCs surface, it is still unclear why NiAl (FeAl) and γ-TiAl (Nb_5Si_3) exhibit such different oxidation behaviors. In addition, the general microscopic selective oxidation mechanism of the IMCs is still lacking. In this paper, we have performed *ab initio* thermodynamics investigation on the selective oxidation behaviors of the binary IMCs surfaces and the surface phase diagrams (SPDs) are presented in the end, which provide a clear physical picture for the above issues.

II. COMPUTATIONAL METHOD AND MODELS

All the calculations are carried out with the Vienna *ab initio* simulation package (VASP) (Refs. 16–18) based on the density-functional theory (DFT),[19,20] employing projector augmented wave (PAW) potentials[21,22] and the PW91 (Ref. 23) generalized gradient approximation (GGA) exchange-correlation functional including spin polarized for magnetic systems. The crystal structures of bulk NiAl and FeAl with B2 structure, γ-TiAl with $L1_0$ structure and α-Nb_5Si_3 with $D8_1$ structure are shown in Fig. 1. For the study of O/NiAl(100) and O/FeAl(100) systems, we use an array of symmetric atomic slabs consisting of nine alternating Al and Ni(Fe) layers separated by a vacuum region equivalent to 11 layers. For the O/γ-TiAl(111) systems, we use an asymmetric slab of seven metal layers separated by a vacuum region equivalent to seven metal layers. For the O/Nb_5Si_3(001) systems, we use a symmetric slab consisting of at least nine metal layers plus at least 15 Å of vacuum layer. A cutoff energy of 400 eV and a $9\times9\times1$ Monkhorst-Pack k points for the surface models are used. An extensive check of the reliability of our calculations may be found in our earlier works.[15,24–27]

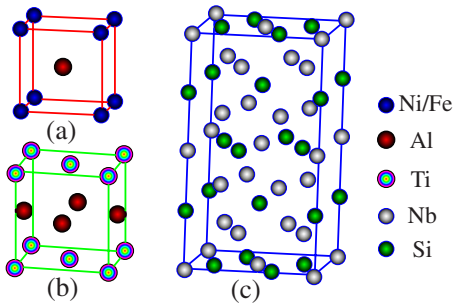

FIG. 1. (Color online) The crystal structures of bulk. (a) NiAl and FeAl with B2 structure, (b) γ-TiAl with $L1_0$ structure, and (c) α-Nb_5Si_3 with $D8_1$ structure.

The thermodynamics calculation involved follows the scheme of previous works.[15,28–33] To evaluate the thermodynamic stability of a given binary (A_mB_n) IMCs surface, it is necessary to determine its corresponding surface-energy γ which is defined as

$$\gamma = \frac{1}{S_0}[E_{slab} - N_A\mu_A - N_B\mu_B - N_O\mu_O - PV - TS], \quad (1)$$

where S_0 is the surface area, E_{slab} is the total energy of the slab, N_A, N_B, and N_O denote the number of A, B, and oxygen atoms in the slab. The chemical potential of A, B, and oxygen are represented by μ_A, μ_B, and μ_O, respectively. We will omit the PV term (P and V are the pressure and volume) and TS term (T and S are temperature and entropy of the system), because these two contributions are negligibly small.[31,32] Invoking equilibrium with IMCs (A_mB_n) bulk ($m\mu_A + n\mu_B = \mu^{bulk}_{A_mB_n}$), two *independent* chemical potentials are sufficient to describe the stability of different surfaces. Therefore, the surface-energy γ can be rewritten as

$$\gamma = \frac{1}{S_0}\left[E_{slab} - \frac{1}{m}N_A\mu^{bulk}_{A_mB_n} - \left(N_B - \frac{n}{m}N_A\right)\mu_B - N_O\mu_O\right]. \quad (2)$$

In order to avoid the formation of metal A and B phases, the chemical potentials must follow $\mu_A \le \mu^{bulk}_A$ and $\mu_B \le \mu^{bulk}_B$. Using equilibrium with IMCs (A_mB_n) bulk ($m\mu_A + n\mu_B = \mu^{bulk}_{A_mB_n}$), the chemical potential of B μ_B varies between $\frac{1}{n}(\mu^{bulk}_{A_mB_n} - m\mu^{bulk}_A) \le \mu_B \le \mu^{bulk}_B$. The upper limit of chemical potential of oxygen is determined by the O_2 molecule, so that $\mu_O \le \frac{1}{2}E^{total}_{O_2}$. Using the *ab initio* computed total energies of bulk A_mB_n, bulk A (A=Ni, Fe, Ti, or Nb), bulk B (B=Al or Si) and molecular O_2, we can obtain the chemical-potential range of O and B, $\mu_O \le -4.89$ eV, -5.05 eV $\le \mu_{Al} \le -3.69$ eV for O/NiAl(100) systems and -4.43 eV $\le \mu_{Al} \le -3.69$ eV for O/FeAl(100) systems, -4.51 eV $\le \mu_{Al} \le -3.69$ eV for O/γ-TiAl(111) systems, and -7.17 eV $\le \mu_{Si} \le -5.43$ eV for O/Nb_5Si_3(001) systems, respectively.

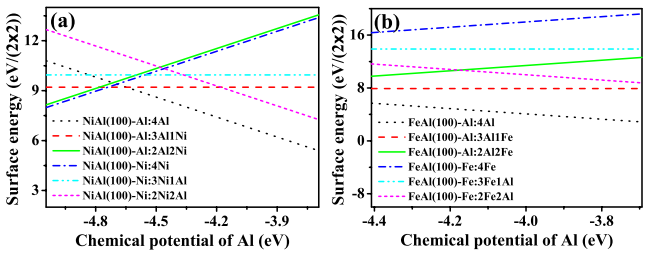

FIG. 2. (Color online) Surface energies of the clean (a) NiAl(100) and (b) FeAl(100) surfaces with the different surface terminations as the functions of μ_{Al}. NiAl(100)-Al:4Al, NiAl(100)-Ni:4Ni, NiAl(100)-Al:3Al1Ni, NiAl(100)-Al(Ni):2Al2Ni, and NiAl(100)-Ni:3Ni1Al denote the NiAl(100)-(2×2) surface with terminations of a pure Al layer, a pure Ni layer, and a mixed Al: Ni occupation at the ratio of 3:1, 1:1, and 1:3 based on the consideration of the antisites defects on both pure Al and Ni layers, respectively. It is the same for FeAl(100) surface.

III. RESULTS AND DISCUSSION

A. Clean surfaces

To investigate the oxygen adsorption on IMCs surfaces, the properties of their clean surfaces should be examined first. The surface energies of the clean NiAl(100)-(2×2) and FeAl(100)-(2×2) surfaces with different surface terminations as the functions of μ_{Al} are shown in Figs. 2(a) and 2(b), respectively. From Fig. 2(a), it can be found that the most stable clean NiAl(100) surface is either a pure Ni or an pure Al terminated surface under Ni- or Ai-rich conditions, it might also be a mixed Ni and Al termination surface in the region between, which indicates that the above three different exclusive surface terminations can be formed in the different μ_{Al} region. In the experiments, the existence of the pure Al termination surface,[34] the pure Ni termination surface,[35,36] and the mixed Al-rich layer with antisite Ni termination surface[36–38] were observed as well in the high-temperature annealing situation for the clean NiAl(100) surface. The above seemingly contradictory findings in the different experiments can be explained explicitly according to our results in Fig. 2(a). For the clean FeAl(100) surface as shown in Fig. 2(b), it can be seen that an Al-terminated surface is the most stable one over the entire range of μ_{Al}, which is in good agreement with the experiment results that the pure Al top layer is stable under normal and even Fe-rich conditions.[36,39]

For the clean γ-TiAl(111) surface, we have examined five possible surface terminations with different surface defects including both Al and Ti antisites. The surface energies of the clean γ-TiAl(111)-(2×2) surface with different surface defects as the functions of μ_{Al} are shown in Fig. 3(a). It can be seen that the γ-TiAl(111) surface with one Al antisite is the most stable over almost the entire range of μ_{Al}, which suggests that one Al antisite can segregate to the top surface easily. Accordingly, the clean surface may be the γ-TiAl(111)-1Al surface. Furthermore, it can also be found that the pure γ-TiAl(111) surface and γ-TiAl(111) surface with two Al antisites are the most stable under Ti- and Al-rich conditions, respectively. For the α-Nb_5Si_3 with $D8_1$

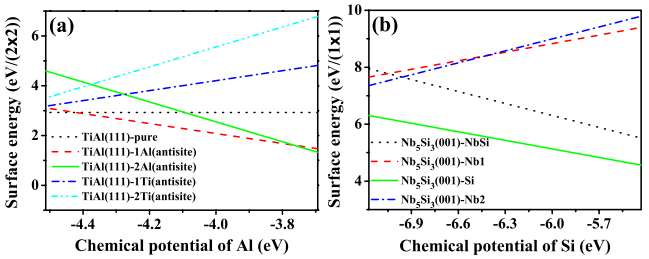

FIG. 3. (Color online) Surface energies of the clean surface (a) γ-TiAl(111) and (b) $Nb_5Si_3(001)$ surfaces with the different surface terminations as the functions of μ_{Al} and μ_{Si}, respectively. TiAl(111), TiAl(111)-1Al(Ti), and TiAl(111)-2Al(Ti) represent the pure γ-TiAl(111)-(2×2) surface and the γ-TiAl(111)-(2×2) surface with one and with two Al(Ti) antisite defects, respectively. $Nb_5Si_3(001)$-NbSi, $Nb_5Si_3(001)$-Nb1, $Nb_5Si_3(001)$-Si, and $Nb_5Si_3(001)$-Nb2 denote the $Nb_5Si_3(001)$-(1×1) surface with terminations of NbSi, Nb, Si, and Nb, respectively.

structure,[25] the surface energies of the clean $Nb_5Si_3(001)$-(1×1) surface with different surface terminations as the functions of μ_{Si} are shown in Fig. 3(b). It is obvious that the surface energy of $Nb_5Si_3(001)$ surface with a Si surface termination is the lowest over the entire range of μ_{Si}, which indicates that the most stable clean surface is a Si-terminated surface. A common feature can be seized from Figs. 2 and 3 that, under the most situations, the simple metal (SM) atoms prefer segregation to the surface relative to the transition-metal (TM) atoms perhaps because the *sp* electrons of SM are more extended than the *d* electrons of TM, which compensates for the discontinuity of the charge near the clean surface.

B. Sustained complete selective oxidation

With the above knowledge, we have examined oxygen adsorption on all the possible surface terminations of the IMCs surfaces. The SPDs for O/NiAl(100) and O/FeAl(100) systems as the functions of μ_{Al} and μ_O are shown in Figs. 4(a) and 4(b), respectively. For O/NiAl(100) systems in Fig. 4(a), under the O-poor conditions, the most stable configurations are the clean surfaces. Concretely, it corresponds to either the pure Ni- or Al-terminated surface under Ni- or Al-rich conditions, while in the region between the mixed Ni

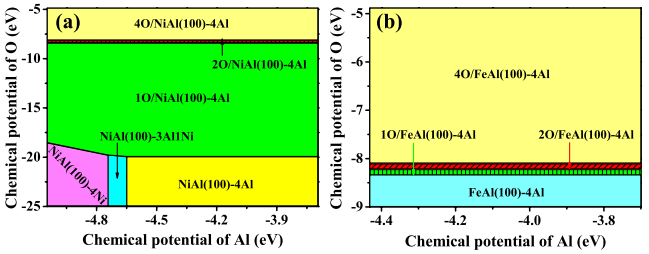

FIG. 4. (Color online) Surface phase diagrams for (a) the O/NiAl(100) and (b) the O/FeAl(100) systems as the functions of μ_{Al} and μ_O. 1O, 2O, and 4O represent one, two, three, and four oxygen atoms adsorption on the IMCs surface, corresponding to 0.25, 0.50, and 1.0 monolayer (ML) oxygen coverage, respectively.

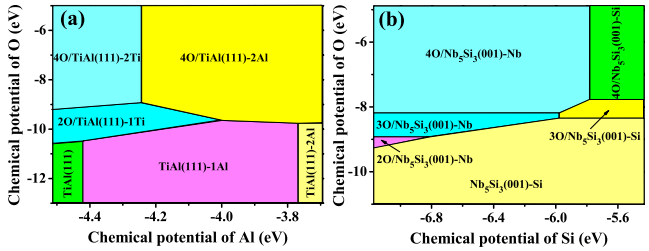

FIG. 5. (Color online) Surface phase diagrams for (a) the O/γ-TiAl(111) and (b) the O/$Nb_5Si_3(001)$ systems as the functions of μ_{Al} and μ_O as well as μ_{Si} and μ_O, respectively. 2O, 3O, and 4O represent two, three, and four oxygen atoms adsorption on the IMCs surface, corresponding to 0.50, 0.75, and 1.0 ML oxygen coverage, respectively.

and Al surface manifests. This is in good agreement with the results shown in Fig. 2(a). Under the O-rich conditions, the most stable configurations are the oxygen adsorption on Al-terminated NiAl(100)-4Al surfaces from low- to high-oxygen coverage, which implies that O can induce complete Al surface segregation even under Ni-rich conditions. It should be noted that under O-poor and Ni-rich conditions, the Ni-terminated NiAl(100)-4Ni surface is the most stable surface, which seems to be easy to form O-Ni oxide layer upon oxygen adsorption intuitively. However, from the thermodynamics point of view in Fig. 4(a), it is the O-Al layer that is the most stable configuration under O-rich conditions, which indicates that O can strongly enhance Al surface segregation, explaining the growth of pure alumina layer in the experiment.[6–8] It also leads to the sustained complete selective oxidation of Al on NiAl(100) surface under O-rich conditions.

For O/FeAl(100) systems in Fig. 4(b), under the O-poor conditions, the most stable configuration is FeAl(100)-4Al, which is a complete Al layer surface. This is also in good agreement with the results shown in Fig. 2(b). Under the O-rich conditions, similar to the O/NiAl(100) systems, the most stable structures are the oxygen adsorption on Al-terminated FeAl(100)-4Al surfaces from low to high-oxygen coverage, in agreement with the formation of pure alumina layer in the experiment.[6,9] Comparison with Figs. 4(a) and 4(b), it can be found that under O-rich conditions the SPDs of O/NiAl(100) and O/FeAl(100) possess a common feature that both of them are uniform over the entire range of μ_{Al}, which corresponds to the sustained complete selective oxidation in the experiment.

C. Nonsustained partial selective oxidation

For O/γ-TiAl(111) systems, the corresponding SPD for oxygen adsorption on the γ-TiAl(111) surfaces with different Al and Ti antisites as the functions of μ_{Al} and μ_O is shown in Fig. 5(a). Under the O-poor conditions, the clean surface is the most stable system. Under the O-rich and high-μ_{Al} conditions, the 4O/γ-TiAl(111)-2Al surface is the most stable configuration, which indicates that O can induce complete Al surface segregation. While under the O-rich and low-μ_{Al} conditions, the 2O/γ-TiAl(111)-1Ti surface is the

most stable configuration. With increasing μ_O, the 4O/γ-TiAl(111)-2Ti surface becomes the most stable configuration, which indicates that O can also induce complete Ti surface segregation. Comparing the phase area of the SPD in Fig. 5(a), it can be seen that the area of 4O/γ-TiAl(111)-2Al is larger than that of 4O/γ-TiAl(111)-2Ti, which suggests the former has a slight thermodynamics advantage. Furthermore, the μ_{Al} in γ-TiAl bulk is about in middle of the whole range of μ_{Al}. Therefore, the slight thermodynamics advantage of 4O/TiAl(111)-2Al system in the middle of μ_{Al} as shown in Fig. 5(a) can explain the selective oxidation of Al at the first stage of oxidation process in the experiments.[10–12] As mentioned above, the element Al is first consumed and depleted gradually by the initial selective oxidation, after that, the element Ti becomes enriched, indicating that the μ_{Al} turns from high to low value. In such a situation, the 4O/TiAl(111)-2Ti system becomes the most stable configuration as shown in Fig. 5(a) under the O-rich and low-μ_{Al} conditions. That is, it turns to Ti-rich condition as the consumption of Al by the initial slight selective oxidation, which induces the oxidation of Ti element easily in turn. Hence, both Al and Ti elements can be oxidized reiteratively under their advantageous conditions, resulting in the competition between Al and Ti elements in the oxidation process, explaining the simultaneous oxidation of the both metal elements in the experiment.[11,12]

For the O/Nb_5Si_3(001) systems, the SPD for oxygen adsorption on the Nb_5Si_3(001) surfaces with different surface terminations as the functions of μ_{Si} and μ_O is shown in Fig. 5(b). Under the O-poor conditions, the Si-terminated Nb_5Si_3(001) surface is the most stable. Intuitively, it seems to be easy to form O-Si oxide layer upon oxygen adsorption. However, under the O-rich conditions, similar to O/γ-TiAl(111) systems, the SPD is also divided into two parts. The large part corresponds to the O-adsorbed Nb-terminated surface, indicating that O can induce complete Nb surface segregation, while the small part of SPD corresponds to the O-adsorbed Si-terminated surface. In addition, the phase area of the 4O/Nb_5Si_3-Nb is much larger than that of the 4O/Nb_5Si_3-Si as shown in Fig. 5(b). Consequently, there exists a competition between Nb and Si elements in the oxidation process, resulting in the formation of the mixture of main Nb_2O_5 and a little SiO_2 in the experiment.[13] Comparison with Figs. 5(a) and 5(b), a common feature can be retrieved that under the O-rich conditions the SPDs of the O/γ-TiAl(111) and the O/Nb_5Si_3(001) systems are divided into two parts over the entire range of μ_{Al} and μ_{Si}, which corresponds to the nonsustained partial selective oxidation in the experiment.

D. General microscopic thermodynamics oxidation mechanism

When one binary IMC is oxidized, does it occur sustained selective oxidation or not? As is known, the initial oxidation of a binary (A_mB_n) IMCs surface can consume one element, supposed to be B, in the formation of its oxide, which results in the richness of the other element A, corresponding to the decrease in the μ_B in the oxidation process. For the SPDs of the O/NiAl(100) and O/FeAl(100) systems shown in Fig. 4, under O-rich conditions the formation of O-Al oxide layers are always the most stable structures under from Al-rich to Al-poor conditions, which indicates that oxygen can always oxidize Al selectively for a long time. This corresponds to the sustained complete selective oxidation of Al, which explains why the continuous coherent Al_2O_3 film can be easily formed on the corresponding IMCs surfaces.[6–9] In contrast, for the SPDs of the O/γ-TiAl(111) and the O/Nb_5Si_3(001) systems shown in Fig. 5, under O-rich conditions it is impossible to form a single oxide layer under from Al(Si)-rich to Al(Si)-poor conditions because of the competition behavior between two elements of a binary IMCs. This corresponds to the nonsustained partial selective oxidation behavior of the IMCs surface, which explains the formation of the mixed oxides on the corresponding IMCs surface through long term oxidation.[11–13]

From above analysis and comparison, the sustained selective oxidation of IMCs surfaces can be seen as one element in IMCs is always selective oxidized over the whole range of μ_B in the SPD and vice versa. Therefore, from the thermodynamics point of view, we can conclude a general microscopic thermodynamics oxidation mechanism that a uniform single-phase SPD (type I) and a nonuniform double-phase SPD (type II) under O-rich conditions correspond to the sustained complete selective oxidation and the nonsustained partial selective oxidation, respectively. Accordingly, using this microscopic oxidation mechanism, one can easily judge and predict the oxidation behavior of arbitrary binary IMCs surfaces in the thermodynamics viewpoint.

IV. CONCLUSION

In summary, based on *ab initio* DFT and the thermodynamics calculations we have investigated the stability of the clean IMCs surfaces and the selective oxidation behaviors on their surfaces. The obtained properties of the clean NiAl(100), FeAl(100), γ-TiAl(111), and Nb_5Si_3(001) surfaces are in good agreement with the relevant experiments. The SPDs of the O/NiAl(100), O/FeAl(100), O/γ-TiAl(111), and the O/Nb_5Si_3(001) systems are also presented, which suggest the existence of two types of SPDs and explain oxidation experimental results successfully. More importantly, the general microscopic thermodynamics oxidation mechanism can be found that under O-rich conditions a uniform single-phase SPD (type I) and a nonuniform double-phase SPD (type II) correspond to the sustained complete selective oxidation and the nonsustained partial selective oxidation, through which one can easily judge and predict the oxidation behaviors of arbitrary binary IMCs surfaces. More generally, our useful physical concepts and approach on the oxidation of IMCs surfaces are expected to be also applicable to many other reactions such as nitrification and sulphuration of IMCs surfaces.

This work was supported by the National Excellent Doctoral Dissertations Foundation under Grant No. 200334 and the National Natural Science Foundation of China under Grants No. 50871071 and No. 50771004. Work of the first author (S.Y.L.) was supported by the Innovation Foundation of BUAA for Ph.D. Graduates.

*shangjx@buaa.edu.cn
†xuhb@buaa.edu.cn

[1] A. Stierle, F. Renner, R. Streitel, H. Dosch, W. Drube, and B. C. Cowie, Science **303**, 1652 (2004).
[2] G. Kresse, M. Schmid, E. Napetschnig, M. Shishkin, L. Köhler, and P. Varga, Science **308**, 1440 (2005).
[3] C. T. Liu, J. Stringer, J. N. Mundy, L. L. Horton, and P. Angelini, Intermetallics **5**, 579 (1997).
[4] N. S. Stoloff, C. T. Liu, and S. C. Deevi, Intermetallics **8**, 1313 (2000).
[5] M. P. Brady and P. F. Tortorelli, Intermetallics **12**, 779 (2004).
[6] R. Franchy, Surf. Sci. Rep. **38**, 195 (2000).
[7] R. P. Blum, D. Ahlbehrendt, and H. Niehus, Surf. Sci. **396**, 176 (1998).
[8] A. Stierle, V. Formoso, F. Comin, G. Schmitz, and R. Franchy, Physica B **283**, 208 (2000).
[9] H. Graupner, L. Hammer, K. Heinz, and D. M. Zehner, Surf. Sci. **380**, 335 (1997).
[10] V. Maurice, G. Despert, S. Zanna, M. P. Bacos, and P. Marcus, Nature Mater. **3**, 687 (2004).
[11] V. Maurice, G. Despert, S. Zanna, M. P. Bacos, and P. Marcus, Surf. Sci. **596**, 61 (2005).
[12] V. Maurice, G. Despert, S. Zanna, P. Josso, M. P. Bacos, and P. Marcus, Acta Mater. **55**, 3315 (2007).
[13] E. S. K. Menon, M. G. Mendiratta, and D. M. Dimiduk, in *Structural Intermetallics*, edited by K. J. Hemker, D. M. Dimiduk, H. Clemens, R. Darolia, H. Inui, J. M. Larsen, K. Sikka, M. Thomas, and J. D. Whittenberger (TMS, The Minerals, Metals, and Materials Society, 2001), pp. 591–600.
[14] A. Y. Lozovoi, A. Alavi, and M. W. Finnis, Phys. Rev. Lett. **85**, 610 (2000).
[15] S. Y. Liu, J. X. Shang, F. H. Wang, and Y. Zhang, Phys. Rev. B **79**, 075419 (2009).
[16] G. Kresse and J. Hafner, Phys. Rev. B **48**, 13115 (1993).
[17] G. Kresse and J. Furthmüller, Phys. Rev. B **54**, 11169 (1996).
[18] G. Kresse and J. Furthmüller, Comput. Mater. Sci. **6**, 15 (1996).
[19] P. Hohenberg and W. Kohn, Phys. Rev. **136**, B864 (1964).
[20] W. Kohn and L. J. Sham, Phys. Rev. **140**, A1133 (1965).
[21] P. E. Blöchl, Phys. Rev. B **50**, 17953 (1994).
[22] G. Kresse and D. Joubert, Phys. Rev. B **59**, 1758 (1999).
[23] J. P. Perdew, J. A. Chevary, S. H. Vosko, K. A. Jackson, M. R. Pederson, D. J. Singh, and C. Fiolhais, Phys. Rev. B **46**, 6671 (1992).
[24] S. Y. Liu, J. X. Shang, F. H. Wang, and Y. Zhang, J. Phys.: Condens. Matter **21**, 225005 (2009).
[25] Y. Chen, J. X. Shang, and Y. Zhang, Phys. Rev. B **76**, 184204 (2007).
[26] Y. Chen, J. X. Shang, and Y. Zhang, J. Phys.: Condens. Matter **19**, 016215 (2007).
[27] Y. Chen, T. Hammerschmidt, D. G. Pettifor, J. X. Shang, and Y. Zhang, Acta Mater. **57**, 2657 (2009).
[28] G. X. Qian, R. M. Martin, and D. J. Chadi, Phys. Rev. B **38**, 7649 (1988).
[29] J. E. Northrup, Phys. Rev. Lett. **62**, 2487 (1989).
[30] F. H. Wang, P. Krüger, and J. Pollmann, Phys. Rev. B **64**, 035305 (2001).
[31] K. Reuter and M. Scheffler, Phys. Rev. B **65**, 035406 (2001).
[32] J. R. Kitchin, K. Reuter, and M. Scheffler, Phys. Rev. B **77**, 075437 (2008).
[33] H. Z. Zhang and S. Q. Wang, Acta Mater. **55**, 4645 (2007).
[34] H. L. Davis and J. R. Noonan, Mater. Res. Soc. Symp. Proc. **83**, 3 (1987).
[35] A. Stierle, V. Formoso, F. Comin, and R. Franchy, Surf. Sci. **467**, 85 (2000).
[36] R. P. Blum, D. Ahlbehrendt, and H. Niehus, Surf. Sci. **366**, 107 (1996).
[37] D. R. Mullins and S. H. Overbury, Surf. Sci. **199**, 141 (1988).
[38] W. D. Roos, J. du Plessis, G. N. van Wyk, E. Taglauer, and S. Wolf, J. Vac. Sci. Technol. A **14**, 1648 (1996).
[39] L. Hammer, W. Meier, V. Bulum, and K. Heinz, J. Phys.: Condens. Matter **14**, 4145 (2002).